

# Entanglement spectroscopy with a depth-two quantum circuit

Yiğit Subaşı, Lukasz Cincio, and Patrick J. Coles

*Theoretical Division, Los Alamos National Laboratory, Los Alamos, NM 87545, USA.*

Noisy intermediate-scale quantum (NISQ) computers have significant decoherence, limiting the depth of circuits that can be implemented on them. A strategy for NISQ algorithms is to reduce the circuit depth at the expense of increasing the qubit count. Here, we exploit this trade-off for an application called entanglement spectroscopy, where one computes the entanglement of a state  $|\psi\rangle$  on systems  $AB$  by evaluating the Rényi entropy of the reduced state  $\rho_A = \text{Tr}_B(|\psi\rangle\langle\psi|)$ . For a  $k$ -qubit state  $\rho(k)$ , the Rényi entropy of order  $n$  is computed via  $\text{Tr}(\rho(k)^n)$ , with the complexity growing exponentially in  $k$  for classical computers. Johri, Steiger, and Troyer [PRB **96**, 195136 (2017)] introduced a quantum algorithm that requires  $n$  copies of  $|\psi\rangle$  and whose depth scales linearly in  $k * n$ . Here, we present a quantum algorithm requiring twice the qubit resources ( $2n$  copies of  $|\psi\rangle$ ) but with a depth that is independent of both  $k$  and  $n$ . Surprisingly this depth is only two gates. Our numerical simulations show that this short depth leads to an increased robustness to decoherence.

## I. INTRODUCTION

Quantum computers promise exponential speedups for various applications, such as simulation of quantum systems [1]. Near-term devices, referred to as noisy intermediate-scale quantum (NISQ) computers [2], are not yet in the regime of realizing these speedups, although quantum supremacy [3, 4] for a specially designed academic problem may be coming soon. Nevertheless, the question of what NISQ computers may be useful for remains an interesting one [2].

Decoherence and gate fidelity continue to be an important issues for NISQ devices [5]. Ultimately these issues limit the depth of algorithms that can be implemented on these computers and increase the computational error for short-depth algorithms. Furthermore, NISQ computers do not currently have enough qubits to fully leverage the benefit of quantum error-correcting codes [6, 7]. This highlights the need for strategies to reduce the depth of quantum algorithms in order to avoid the accumulation of errors [8].

One such strategy notes that there is often a trade-off between the circuit depth and the number of qubits involved in one’s algorithm [9]. Namely, increasing the number of qubits can lead to shorter depth. Recently, industry quantum computers seem to be increasing their qubit counts relatively rapidly, although these qubits are noisy [5]. So this strategy may be fruitful in the near term (i.e., before error correction is possible). A second strategy notes that quantum algorithms can be hybridized (i.e., made into quantum-classical algorithms) whereby part of the computation is done on a classical computer [10, 11]. This reduces the load for the (error-prone) quantum computer.

In this paper, we employ both of these strategies to dramatically reduce the circuit depth for a particular application called entanglement spectroscopy [12–14]. Here one computes the entanglement of a pure bipartite quantum state  $|\psi\rangle$  on systems  $AB$  by measuring various entropies of the reduced state  $\rho_A = \text{Tr}_B(|\psi\rangle\langle\psi|)$ . The entanglement in  $|\psi\rangle$  is completely characterized by

the eigenvalues of  $\rho_A$ . Li and Haldane noted that the largest eigenvalues of  $\rho_A$  contain more universal signatures than the von Neumann entropy alone [12]. They introduced the concept of entanglement spectrum, writing  $\rho_A = \exp(-H_E)$  as the exponential of the “entanglement Hamiltonian” so that the largest eigenvalues correspond to the lowest energies of  $H_E$ . As noted, e.g., in [15], the integer Rényi entropies of  $\rho_A$  can be used to reconstruct the largest eigenvalues of  $\rho_A$ .

Entanglement spectroscopy will be important in the future when quantum computers are large enough to perform quantum simulation of many-body systems [16]. Imagine that  $|\psi\rangle$  is the output of the simulation, and one wants to characterize this state with a figure-of-merit quantifying entanglement. Since  $|\psi\rangle$  is already in quantum form (as opposed to a vector of amplitudes, as one would store it on a classical computer), one can directly act with a quantum gate sequence and measurements on  $|\psi\rangle$  to compute this figure-of-merit.

The Rényi entropy of order  $n$  is defined as

$$S_n(\rho) = \frac{1}{1-n} \log(R_n(\rho)) \quad (1)$$

where

$$R_n(\rho) = \text{Tr}(\rho^n), \quad (2)$$

and we consider  $n \geq 2$  to be an integer in this work. Suppose that  $\rho(k)$  is a  $k$ -qubit state. Since  $\rho(k)$  is a  $2^k \times 2^k$  matrix, the complexity of computing  $\rho(k)^n$  and hence  $S_n(\rho(k))$  grows exponentially with  $k$  for a classical computer. In contrast, Johri et al. [15] introduced a quantum algorithm that computes  $S_n(\rho(k))$  with complexity growing bilinearly in  $k$  and  $n$ , i.e., with the product  $k * n$ . Their algorithm generalized the well-known Swap Test for computing purity  $\text{Tr}(\rho^2)$  and state overlap. That is, by replacing the controlled-swap operator in the Swap Test with a controlled-permutation operator, their algorithm can compute  $\text{Tr}(\rho^n)$  for integer  $n \geq 2$ . This algorithm is shown in Fig. 1.

In this work, we propose an alternative quantum algorithm for entanglement spectroscopy. Our algorithm dramatically shortens the depth relative to that of Ref. [15],

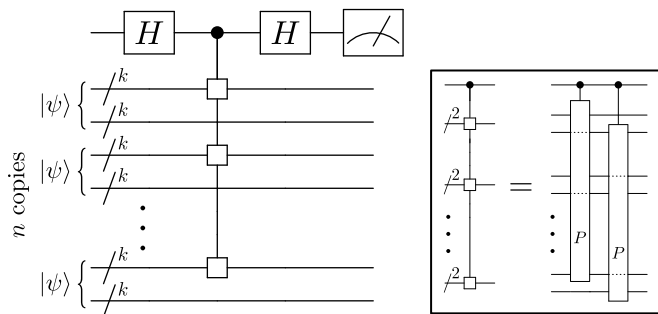


FIG. 1. Algorithm presented in [15] to compute  $\text{Tr}(\rho_A^n)$  for integer  $n \geq 2$ . Here,  $\rho_A$  contains  $k$  qubits and is the reduced state of  $|\psi\rangle$  (containing  $2k$  qubits). Two Hadamards sandwich a controlled-permutation gate acting on  $n$  copies of  $|\psi\rangle$ . The controlled-permutation gate is expanded in the inset, for the special case of  $k = 2$ . Each controlled- $P$  gate is then decomposed into  $n$  controlled-swaps, which in turn are written in terms of CNOTs and one-body gates [17]. This shows that the algorithm's gate depth grows in proportion to  $k * n$ . Here we assumed for simplicity that the state  $\rho_A$  contains half of the qubits in  $|\psi\rangle$ . The generalization to arbitrary bipartition is straightforward.

at the expense of requiring more qubits and more classical post-processing. Namely, Ref. [15] requires  $n$  copies of  $|\psi\rangle$ , with a circuit depth growing with  $k * n$ . At the end a single ancilla qubit is measured to compute the expectation value of the Pauli- $Z$  operator. In contrast, our algorithm requires  $2n$  copies of  $|\psi\rangle$ , while our circuit depth is, surprisingly, independent of both  $k$  and  $n$ . Furthermore, this depth is only two quantum gates. At the end all qubits are measured and the post-processing of our algorithm grows in proportion to  $k * n$ . In this way we have transferred some of the complexity from quantum into classical computation. For NISQ devices, it is always better to push complexity onto classical computers, which are essentially error free.

At the core of our algorithm is an alternative approach to computing the expectation value of an operator  $M$ . It is well known that the Hadamard Test can be used to find  $\langle\psi|M|\psi\rangle$  by implementing the controlled- $M$  gate, see Fig. 2(a). In this work, we note that  $|\langle\psi|M|\psi\rangle|^2$  can be computed by implementing  $M$  instead of controlled- $M$ , if one allows for two copies of  $|\psi\rangle$ . We call the latter approach the Two-Copy Test, and it is depicted in Fig. 2(b). For computing the Rényi entropies in Eq. (1),  $M$  is set to be the cyclic permutation operator.

In what follows, we first give some background, including the connection between the permutation operator and the integer Rényi entropies as well as the connection between these entropies and the largest eigenvalues of the state. We then present our main result: a quantum circuit with a depth of two gates for computing the integer Rényi entropies. Finally, we numerically simulate our circuit as well as the circuit in Fig. 1, and we discuss how our circuit leads to increased robustness to noise, partic-

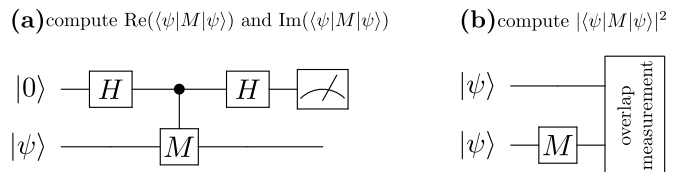


FIG. 2. Two different strategies for computing an operator's expectation value. (a) The Hadamard Test involves applying controlled- $M$  and requires one copy of  $|\psi\rangle$  and one ancilla. By varying the final measurement in the  $xy$  plane of the Bloch sphere, one can extract linear combinations of  $\text{Re}(\langle\psi|M|\psi\rangle)$  and  $\text{Im}(\langle\psi|M|\psi\rangle)$ . (b) Here we invoke a different algorithm that we call the Two-Copy Test, which requires two copies of  $|\psi\rangle$ . This algorithm applies  $M$  to one of the two copies and then measures the overlap between the copies, giving  $|\langle\psi|M|\psi\rangle|^2$ .

ularly when the readout error is small compared to other sources of noise.

## II. BACKGROUND

### A. Rényi entropies via the permutation operator

Nonlinear functions of a state  $\rho$  can be obtained by evaluating linear expectation values on multiple copies of  $\rho$ . One of the most well-known examples is the swap trick, which uses two copies of  $\rho$  to evaluate the purity:

$$\text{Tr}(\rho^2) = \text{Tr}((\rho \otimes \rho)S) \quad (3)$$

where  $S = \sum_{j,k} |jk\rangle\langle kj|$  is the swap operator. This trick generalizes to  $n \geq 2$  copies of  $\rho$  as follows:

$$\text{Tr}(\rho^n) = \text{Tr}(\rho^{\otimes n}P) \quad (4)$$

where

$$\rho^{\otimes n} = \rho \otimes \rho \otimes \dots \otimes \rho \quad (n \text{ times}). \quad (5)$$

Here

$$P = \sum_{j_1, j_2, \dots, j_n} |j_n j_1 j_2 \dots j_{n-1}\rangle\langle j_1 j_2 \dots j_n| \quad (6)$$

is the cyclic permutation operator, permuting the  $n$  subsystems of  $\rho^{\otimes n}$ .

An important property of  $P$  is that it factorizes into a tensor product of permutation operators when acting on a tensor-product Hilbert space. To make this clear, let  $P_k^{(n)}$  denote the permutation operator acting on  $n$  quantum systems, each of which is composed of  $k$  qubits. Suppose that  $Q$  is a composite quantum system composed of  $n$  subsystems:

$$Q = Q^{(1)}Q^{(2)} \dots Q^{(n)}, \quad (7)$$

and that each  $Q^{(i)}$  is composed of  $k$  qubits:

$$Q^{(i)} = Q_1^{(i)} Q_2^{(i)} \dots Q_k^{(i)} \quad (8)$$

where  $Q_j^{(i)}$  denotes the  $j$ -th qubit in the  $i$ -th subsystem,  $Q^{(i)}$ . Then, when  $P_k^{(n)}$  acts on the Hilbert space associated with the  $Q$  system, it can be written as

$$P_k^{(n)} = P_1^{(n)} \otimes P_1^{(n)} \otimes \dots \otimes P_1^{(n)} \quad (k \text{ times}), \quad (9)$$

provided that we order the qubits in the following way

$$Q_1^{(1)} Q_1^{(2)} \dots Q_1^{(n)} \dots Q_k^{(1)} Q_k^{(2)} \dots Q_k^{(n)}. \quad (10)$$

Note that  $P_1^{(n)}$  in (9) is the operator that permutes  $n$  subsystems each of which is composed of one qubit.

## B. Computing eigenvalues from Rényi entropies

In order to exactly compute all eigenvalues  $\{\lambda_i\}$  of the density matrix  $\rho$  of a system of  $k$  qubits, one needs to know all Rényi entropies up to order  $2^k$ . As noted in Ref. [15] these quantities can be related to each other by the Newton-Girard Formula:

$$(x - \lambda_1)(x - \lambda_2) \dots (x - \lambda_N) = \sum_{m=0}^N (-1)^{N-m} e_{N-m} x^m \quad (11)$$

where  $N = 2^k$  is the dimension of  $\rho$  and

$$\begin{aligned} e_0 &= 1 \\ e_1 &= R_1 \\ e_2 &= \frac{1}{2}(e_1 R_1 - R_2) \\ e_3 &= \frac{1}{3}(e_2 R_1 - e_1 R_2 + R_3) \\ e_4 &= \frac{1}{4}(e_3 R_1 - e_2 R_2 + e_1 R_3 - R_4) \\ &\vdots \end{aligned} \quad (12)$$

However, in most cases we are only interested in a small number of largest eigenvalues  $\lambda_1 \geq \lambda_2 \geq \dots \geq \lambda_{n_{\max}}$ . In Ref. [15] it was argued that an approximation to the  $n_{\max}$  largest eigenvalues of  $\rho$  can be obtained by truncating the polynomial on the right hand side of Eq. (11) to that order and solving for the roots. Using this method we can approximately compute  $n_{\max}$  largest eigenvalues of  $\rho$  from the Rényi entropies of order up to  $n_{\max}$ .

## III. MAIN RESULT

Here we present our main result: a circuit for computing the integer Rényi entropies with a depth of only

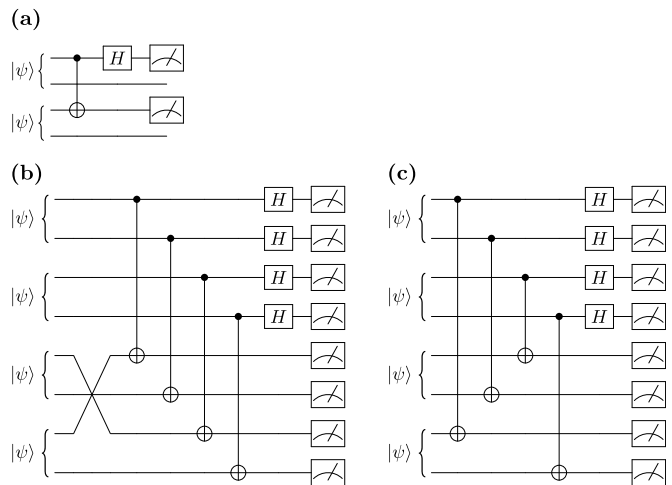


FIG. 3. Circuits for computing  $\text{Tr}(\rho_A^2)$  with a depth of two. The classical post-processing is not shown, but is discussed in the text. (a) Refs. [11, 18] showed that the Bell-basis measurement on two copies of the state computes  $\text{Tr}(\rho_A^2)$ . (b) Our algorithm applied to  $n = 2$  and  $k = 1$ , which is based on the Two-Copy Test shown in Fig. 2. Namely, we feed in two copies of  $|\psi_2\rangle := |\psi\rangle \otimes |\psi\rangle$ , i.e., four copies of  $|\psi\rangle$ , in order to compute  $|\langle \psi_2 | S_A | \psi_2 \rangle|^2$ , where  $S_A$  is the swap operator for the  $A$  subsystems. This involves applying  $S_A$  to one copy of  $|\psi_2\rangle$  and then measuring the overlap with the other copy of  $|\psi_2\rangle$ . The overlap measurement is the Bell-basis measurement, i.e., the same measurement employed in part (a) of this figure. (c) Note that the swap gate simply changes the targets of the subsequent CNOT gates in the circuit. Furthermore, note that all of the CNOTs and Hadamards can be performed in parallel, giving a circuit depth of two.

two quantum gates. We emphasize that our circuit does require access to the full pure state  $|\psi\rangle$  in order to compute the Rényi entropies of the reduced state  $\rho_A = \text{Tr}_B(|\psi\rangle\langle\psi|)$ . For readability, we first illustrate our circuit for the simplest case of computing purity for one-qubit states.

### A. Special case of $n = 2, k = 1$

Suppose  $\rho_A = \text{Tr}_B(|\psi\rangle\langle\psi|)$  is a single-qubit state and one wishes to compute  $\text{Tr}(\rho_A^2)$ . Previous work [11, 18] showed that this can be done via a Bell-basis measurement on two copies of the state, as depicted in Fig. 3(a). This measurement involves applying a CNOT followed by a Hadamard on one of the copies. Finally one applies a classical post-processing as a simple dot product with the probability vector, i.e.,

$$\text{Tr}(\rho_A^2) = \vec{c} \cdot \vec{p} \quad (13)$$

where  $\vec{p} = \{p_{00}, p_{10}, p_{01}, p_{11}\}$  is the probability vector for the measurement outcomes and  $\vec{c} = \{1, 1, 1, -1\}$ .

For  $n = 2$  we recommend employing the aforementioned algorithm in Fig. 3(a). Nevertheless, we show

how the algorithm presented in this paper applies to the  $n = 2$  case in Fig. 3(b). The Two-Copy Test in Fig. 2(b) is the basis of our algorithm. We feed in two copies of  $|\psi_2\rangle := |\psi\rangle \otimes |\psi\rangle$ , i.e., four copies of  $|\psi\rangle$ . We apply the swap operator  $S_A$  to one copy of  $|\psi_2\rangle$ , where the  $A$  subscript indicates that the swap is being applied only to the  $A$  subsystems. Then we measure the overlap with the other copy of  $|\psi_2\rangle$ , which gives:

$$|\langle\psi_2|S_A|\psi_2\rangle|^2 = (\text{Tr}(\rho_A^2))^2. \quad (14)$$

The proof of Eq. (14) is straightforward and is shown below in Eq. (18).

We emphasize that the implementation of the swap gate is trivial since its only effect is to change the ordering of the qubits, as shown in Fig. 3(c). The same effect can be achieved by changing the indices of the target qubits in the CNOTs following the swap gate. The depth of the circuit in Fig. 3(c) is due to the gates that compose the overlap measurement, and this depth is two gates, since the various CNOTs and Hadamards on distinct qubits can be parallelized.

The classical post-processing needed to obtain Eq. (14) from the measurement results in Fig. 3(c) involves taking the dot product with the probability vector  $\vec{p}$ , as in Eq. (13), but with

$$(\text{Tr}(\rho_A^2))^2 = \vec{c} \cdot \vec{p}, \quad \vec{c} = \{1, 1, 1, -1\}^{\otimes 4}. \quad (15)$$

The form of  $\vec{c}$  stated here requires one to reorder the qubits such that each qubit is grouped next to its overlap partner, i.e., each qubit controlling a CNOT in Fig. 3(c) is immediately followed by the qubit being targeted by that CNOT. An explicit form of the post-processing in this case is thus given by:

$$(\text{Tr}(\rho_A^2))^2 = \sum_{j_1, \dots, j_8} (-1)^{j_1 j_7 + j_2 j_6 + j_3 j_5 + j_4 j_8} p_{j_1, \dots, j_8}. \quad (16)$$

### B. Circuit for general $n$ and $k$

Our main result is the circuit in Fig. 4, which generalizes the special case shown in Fig. 3(b). This gives a general algorithm for computing the integer Rényi entropies for  $n \geq 2$ , for states with an arbitrary number of qubits. For simplicity, we assume the number of qubits in subsystems  $A$  and  $B$  are the same and equal to  $k$ , as the extension to arbitrary bipartitions is straightforward. Due to the circuit's generality, we introduce some compact circuit notation in Fig. 4(b) and (c), respectively defining the permutation gate and CNOT gates between multiple pairs of control and target qubits.

Surprisingly, the circuit depth is independent of the problem size, i.e., independent of both  $n$  and  $k$ . One can see this by noting that: (1) the cyclic permutation gate, shown in Fig. 4(b), does not add to the circuit depth since it just reorders the qubits, and (2) the CNOT and

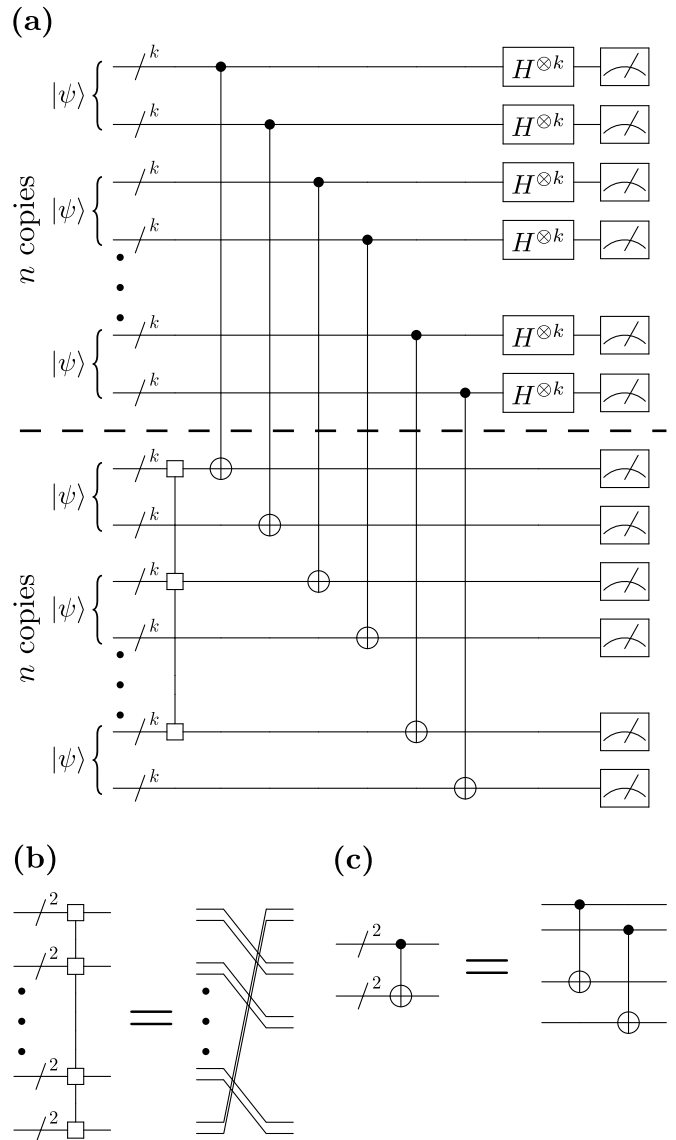


FIG. 4. Circuit for computing the integer Rényi entropies  $S_n(\rho_A)$ , or more precisely  $\text{Tr}(\rho_A^n)$ , for  $n \geq 2$  where  $\rho_A = \text{Tr}_B(|\psi\rangle\langle\psi|)$ . The circuit acts on a total of  $2n$  copies of  $|\psi\rangle$ , or in other words, two copies of  $|\psi_n\rangle := |\psi\rangle^{\otimes n}$ . We employ a compact notation for the cyclic permutation gate and for CNOT gates between multiple pairs of control and target qubits, respectively shown in (b) and (c) for the special case of  $k = 2$ .

Hadamard gates on distinct qubits can be parallelized. The result is a circuit with a depth of two quantum gates.

As noted earlier, the conceptual basis of our algorithm is the Two-Copy Test from Fig. 2(b). We prepare two copies of the state  $|\psi_n\rangle := |\psi\rangle^{\otimes n}$ . We apply the permutation gate  $P_A$  to one of these copies, where the  $A$  subscript indicates that the permutation is applied only to the  $A$  subsystems. Then we measure the overlap with

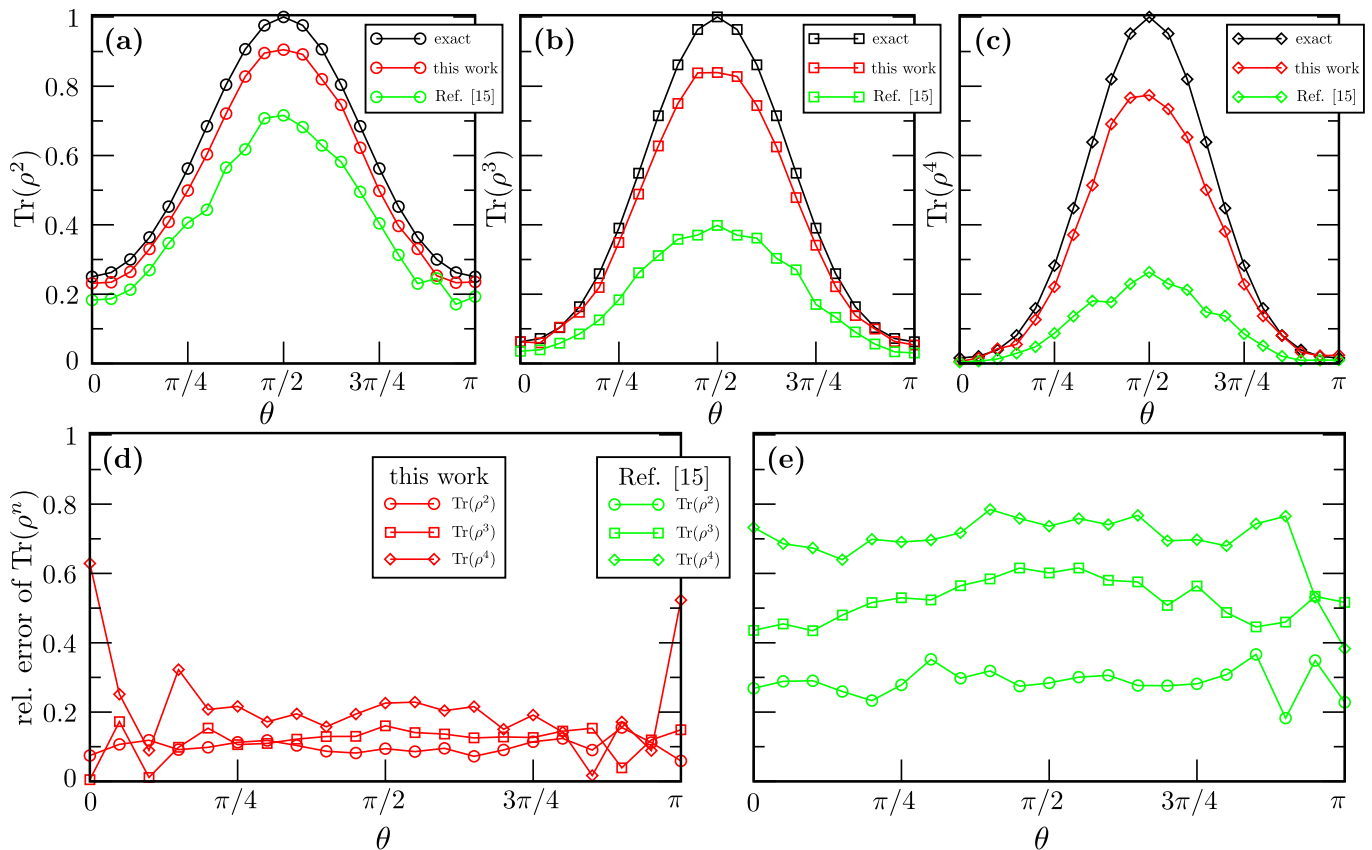


FIG. 5. Numerical simulation of our algorithm and the algorithm in Ref. [15] using QuTiP. For each qubit, the decoherence parameters were set to  $T_1 = T_2 = 200$  in units of gate implementation time, and the measurement readout error was set to 0.5%. Curves are plotted versus the parameter  $\theta$  defined in (21). Plots (a), (b), and (c) show the  $n = 2$ ,  $n = 3$ , and  $n = 4$  cases respectively, including the exact curve (black), the curve associated with the algorithm in Fig. 4 (red), and the curve associated with the algorithm in Fig. 1 (green). The relative error is plotted in (d) and (e) for the algorithms in Fig. 4 and Fig. 1, respectively.

the other copy, giving

$$|\langle \psi_n | P_A | \psi_n \rangle|^2 = (\text{Tr}(\rho_A^n))^2. \quad (17)$$

Taking the logarithm of Eq. (17) and dividing by  $2(1 - n)$  then gives the Rényi entropy  $S_n(\rho_A)$ . The proof of Eq. (17) is simply

$$\begin{aligned} \langle \psi_n | P_A | \psi_n \rangle &= \text{Tr}_{AB}(|\psi_n\rangle\langle\psi_n| P_A) \\ &= \text{Tr}_A(\rho_A^{\otimes n} P_A) \\ &= \text{Tr}(\rho_A^n). \end{aligned} \quad (18)$$

The classical post-processing needed to obtain Eq. (17) from the measurement results is analogous to that discussed previously in Eq. (15), namely

$$(\text{Tr}(\rho_A^n))^2 = \vec{c} \cdot \vec{p}, \quad \vec{c} = \{1, 1, 1, -1\}^{\otimes 2kn}. \quad (19)$$

Again, the form of  $\vec{c}$  here requires a special ordering of the qubits, whereby each qubit that controls a CNOT in Fig. 4 is followed by the target qubit for that CNOT. Hence each vector  $\{1, 1, 1, -1\}$  is associated with a pair of qubits, and there are a total of  $2kn$  qubit pairs in Fig. 4.

#### IV. NUMERICAL SIMULATION

We employed QuTiP [19, 20] (Quantum Toolbox in Python) to simulate the implementation of the algorithm presented in Fig. 4 as well as the algorithm from Ref. [15]. We considered  $k = 1$ , so that  $\rho_A = \text{Tr}_B(|\psi\rangle\langle\psi|)$  is a one-qubit state, and  $n = 2$ ,  $n = 3$ , and  $n = 4$  corresponding to  $\text{Tr}(\rho_A^2)$ ,  $\text{Tr}(\rho_A^3)$ , and  $\text{Tr}(\rho_A^4)$ . In particular, we considered a one-parameter family of states  $|\psi\rangle$  prepared as follows:

$$|\psi\rangle = \text{CNOT}_{AB}(H|0\rangle_A \otimes U(\theta)|0\rangle_B), \quad (20)$$

where  $\text{CNOT}_{AB}$  is a controlled-NOT with  $A$  ( $B$ ) as the control (target) qubit, and

$$U(\theta) := R_z(\theta)R_x(\pi/2). \quad (21)$$

The parameter  $\theta$  determines how much entanglement  $|\psi\rangle$  has and hence how mixed the reduced state  $\rho_A$  is.

Our simulation accounted for relaxation and decoherence due to  $T_1$  and  $T_2$  processes, choosing  $T_1 = T_2 =$

$200t_g$  for each qubit. Here  $t_g$  is the execution time of each quantum gate, which for simplicity we chose to be the same for all 1-qubit gates and CNOT gates. In addition, we accounted for measurement noise, with a readout error of 0.5% for each qubit. We did not model gate imperfections.

The simulation results are shown in Fig. 5. Panels (a), (b), and (c) compare the algorithms in Fig. 4 and Fig. 1 with the exact curve for  $n = 2, 3$ , and 4, respectively. In each case, the algorithm in Fig. 4 gets closer to the exact curve. The relative errors for the two algorithms are shown in panels (d) and (e).

For the particular noise parameters chosen in Fig. 5, it appears that the error increases with  $n$  more rapidly for the algorithm in Fig. 1. Naturally, one expects the error to increase with  $n$  for both algorithms, since the number of state preparations of  $|\psi\rangle$  (each of which has an associated error) increases linearly with  $n$ . In addition, the depth of the algorithm in Fig. 1 increases linearly in  $n$ , while the number of measurements in the algorithm in Fig. 4 increases linearly in  $n$ . As a result, one expects the algorithm in Fig. 1 to be more sensitive to decoherence (due to the increased depth), while the algorithm in Fig. 4 should be more sensitive to readout error (due to the increased number of measurements).

Although we did not model gate imperfections in Fig. 5, we expect them to affect our algorithm less than the algorithm in Fig. 1. This is because, for each CNOT gate that one needs to implement in our algorithm, one needs to implement 8 CNOT gates in the algorithm in

Fig. 1 [17].

## V. CONCLUSIONS

In this work we presented a new quantum algorithm for computing the integer Rényi entropies, which can be used to determine the entanglement spectrum. Relative to the algorithm in [15], our algorithm doubled the number of qubits required but dramatically reduced the quantum gate depth. In doing so, we pushed the quantum gate scaling (which is proportional  $k * n$  for the algorithm in [15]) into the complexity of classical post-processing; hence our algorithm is a hybrid quantum-classical algorithm. As a result, the quantum portion of our algorithm has a depth of only two gates. This makes it ideal for implementations on NISQ computers, whose qubit counts are rapidly growing, but whose qubits remain noisy.

We remark that computing higher order Rényi entropies may be used to compute bounds for von Neumann entropic quantities [21]. We also note that the Two-Copy Test in Fig. 2 for computing the expectation value of an operator  $M$  may be of independent interest, since it avoids implementing a (costly) controlled- $M$  gate as in the Hadamard Test and hence is more amenable to blackbox implementation of  $M$ .

## VI. ACKNOWLEDGEMENTS

YS acknowledges support of the LDRD program at Los Alamos National Laboratory (LANL). LC was supported by the U.S. Department of Energy through the J. Robert Oppenheimer fellowship. PJC was supported by the LANL ASC Beyond Moore's Law project.

- 
- [1] Richard P Feynman. Simulating physics with computers. *International journal of theoretical physics*, 21(6-7):467–488, 1982.
  - [2] John Preskill. Quantum computing in the NISQ era and beyond. *arXiv:1801.00862*, 2018.
  - [3] John Preskill. Quantum computing and the entanglement frontier. *arXiv:1203.5813*, 2012.
  - [4] C Neill, P Roushan, K Kechedzhi, S Boixo, SV Isakov, V Smelyanskiy, R Barends, B Burkett, Y Chen, Z Chen, et al. A blueprint for demonstrating quantum supremacy with superconducting qubits. *arXiv:1709.06678*, 2017.
  - [5] Philip Ball. The era of quantum computing is here. Outlook: cloudy. *Quanta Magazine*, 2018.
  - [6] Austin G Fowler, Matteo Mariantoni, John M Martinis, and Andrew N Cleland. Surface codes: Towards practical large-scale quantum computation. *Physical Review A*, 86(3):032324, 2012.
  - [7] Hao You, Michael R Geller, PC Stancil, et al. Simulating the transverse Ising model on a quantum computer: Error correction with the surface code. *Physical Review A*, 87(3):032341, 2013.
  - [8] Kristan Temme, Sergey Bravyi, and Jay M Gambetta. Error mitigation for short-depth quantum circuits. *Physical review letters*, 119(18):180509, 2017.
  - [9] Anne Broadbent and Elham Kashefi. Parallelizing quantum circuits. *Theoretical computer science*, 410(26):2489–2510, 2009.
  - [10] Jarrod R McClean, Jonathan Romero, Ryan Babbush, and Alán Aspuru-Guzik. The theory of variational hybrid quantum-classical algorithms. *New Journal of Physics*, 18(2):023023, 2016.
  - [11] Lukasz Cincio, Yiğit Subaşı, Andrew T Sornborger, and Patrick J Coles. Learning the quantum algorithm for state overlap. *arXiv:1803.04114*, 2018.
  - [12] Hui Li and F Duncan M Haldane. Entanglement spectrum as a generalization of entanglement entropy: Identification of topological order in non-abelian fractional quantum hall effect states. *Physical Review Letters*, 101(1):010504, 2008.
  - [13] Luigi Amico, Rosario Fazio, Andreas Osterloh, and Vlatko Vedral. Entanglement in many-body systems. *Reviews of Modern Physics*, 80:517–576, 2008.
  - [14] Ryszard Horodecki, Paweł Horodecki, Michał Horodecki, and Karol Horodecki. Quantum entanglement. *Reviews of Modern Physics*, 81(2):865, 2009.

- [15] Sonika Johri, Damian S Steiger, and Matthias Troyer. Entanglement spectroscopy on a quantum computer. *Physical Review B*, 96(19):195136, 2017.
- [16] Norbert M Linke, Sonika Johri, Caroline Figgatt, Kevin A Landsman, Anne Y Matsuura, and Christopher Monroe. Measuring the Rényi entropy of a two-site Fermi-Hubbard model on a trapped ion quantum computer. *arXiv:1712.08581*, 2017.
- [17] Vivek V Shende and Igor L Markov. On the CNOT-cost of Toffoli gates. *Quantum Information and Computation*, 9(5&6):0461–0486, 2009.
- [18] Juan Carlos Garcia-Escartin and Pedro Chamorro-Posada. Swap test and Hong-Ou-Mandel effect are equivalent. *Physical Review A*, 87(5):052330, 2013.
- [19] JR Johansson, PD Nation, and Franco Nori. Qutip: An open-source Python framework for the dynamics of open quantum systems. *Computer Physics Communications*, 183(8):1760–1772, 2012.
- [20] JR Johansson, PD Nation, and Franco Nori. Qutip 2: A Python framework for the dynamics of open quantum systems. *Computer Physics Communications*, 184:1234, 2013.
- [21] Graeme Smith, John A Smolin, Xiao Yuan, Qi Zhao, Davide Girolami, and Xiongfeng Ma. Quantifying coherence and entanglement via simple measurements. *arXiv:1707.09928*, 2017.